

1 **Water adsorption and hygroscopic growth of six anemophilous pollen species: the**
2 **effect of temperature**

3
4 Mingjin Tang,^{1,5,6,*} Wenjun Gu,^{1,5} Qingxin Ma,^{2,5,6,*} Yong Jie Li,³ Cheng Zhong,^{2,5} Sheng Li,^{1,5}
5 Xin Yin,^{1,5} Ru-Jin Huang,^{4,7} Hong He,^{2,5,6} Xinming Wang^{1,5,6}

6
7 ¹ State Key Laboratory of Organic Geochemistry and Guangdong Key Laboratory of
8 Environmental Protection and Resources Utilization, Guangzhou Institute of Geochemistry,
9 Chinese Academy of Sciences, Guangzhou 510640, China

10 ² State Key Joint Laboratory of Environment Simulation and Pollution Control, Research Center
11 for Eco-Environmental Sciences, Chinese Academy of Sciences, Beijing 100085, China

12 ³ Department of Civil and Environmental Engineering, Faculty of Science and Technology,
13 University of Macau, Avenida da Universidade, Taipa, Macau, China

14 ⁴ Key Laboratory of Aerosol Chemistry and Physics, State Key Laboratory of Loess and
15 Quaternary Geology, Institute of Earth and Environment, Chinese Academy of Sciences, Xi'an
16 710061, China

17 ⁵ University of Chinese Academy of Sciences, Beijing 100049, China

18 ⁶ Center for Excellence in Regional Atmospheric Environment, Institute of Urban Environment,
19 Chinese Academy of Sciences, Xiamen 361021, China

20 ⁷ Center for Excellence in Quaternary Science and Global Change, Xi'an 710061, China

21
22 * Correspondence: Mingjin Tang (mingjintang@gig.ac.cn), Qingxin Ma (qxma@rcees.ac.cn)

24 **Abstract**

25 Hygroscopicity largely affects environmental and climatic impacts of pollen grains, one
26 important type of primary biological aerosol particles in the troposphere. However, our knowledge
27 in pollen hygroscopicity is rather limited, and especially the effect of temperature has rarely been
28 explored before. In this work three different techniques, including a vapor sorption analyzer,
29 diffusion reflectance infrared Fourier transform spectroscopy (DRIFTS) and transmission Fourier
30 transform infrared spectroscopy (transmission FTIR) were employed to characterize six
31 anemophilous pollen species and to investigate their hygroscopic properties as a function of
32 relative humidity (RH, up to 95%) and temperature (5 or 15, 25 and 37 °C). Substantial mass
33 increase due to water uptake was observed for all the six pollen species, and at 25 °C the relative
34 mass increase at 90% RH, when compared to that at <1% RH, ranged from ~30 to ~50%, varying
35 with pollen species. It was found that the modified κ -Köhler equation can well approximate mass
36 hygroscopic growth of all the six pollen species, and the single hygroscopicity parameter (κ) was
37 determined to be in the range of 0.034 ± 0.001 to 0.061 ± 0.007 at 25 °C. In-situ DRIFTS
38 measurements suggested that water adsorption by pollen species was mainly contributed by OH
39 groups of organic compounds they contained, and good correlations were indeed found between
40 hygroscopicity of pollen species and the amount of OH groups, as determined using transmission
41 FTIR. Increase in temperature would in general lead to decrease in hygroscopicity, except for
42 pecan pollen. For example, κ values decreased from 0.073 ± 0.006 at 5 °C to 0.061 ± 0.007 at 25 °C
43 and to 0.057 ± 0.004 at 37 °C for populus tremuloides pollen, and decreased from 0.060 ± 0.001 at
44 15 °C to 0.054 ± 0.001 at 25 °C to 0.050 ± 0.002 at 37 °C for paper mulberry pollen.

45

46 **1 Introduction**

47 Primary biological aerosol particles (PBAPs), an important type of aerosol particles in the
48 troposphere, are directly emitted from the biosphere and include pollen, fungal spores, bacteria,
49 viruses, algae, and so on (Després et al., 2012; Fröhlich-Nowoisky et al., 2016). Emission and
50 abundance of PBAPs are quite uncertain, and annual emission fluxes are estimated to be in the
51 range of <10 to ~1000 Tg for total PBAPs and 47-84 Tg for pollen (Després et al., 2012). Pollen,
52 and PBAPs in general, are of great concerns due to their various impacts on the Earth system (Sun
53 and Ariya, 2006; Ariya et al., 2009; Georgakopoulos et al., 2009; Morris et al., 2011; Morris et al.,
54 2014; Fröhlich-Nowoisky et al., 2016). For example, they can be allergenic, infectious or even
55 toxic, affecting the health of human and other species in the ecological systems over different
56 scales (Douwes et al., 2003; Reinmuth-Selzle et al., 2017; Shiraiwa et al., 2017). The geographical
57 dispersion of anemophilous plants largely relies on pollen dispersal, which in turn depends on the
58 emission, transport and deposition of pollen grains; therefore, pollen plays a key role in the
59 evolution of many ecosystems (Womack et al., 2010; Fröhlich-Nowoisky et al., 2016). In addition,
60 PBAPs can serve as giant cloud condensation nuclei (CCN) and ice nucleating particles (INPs),
61 significantly impacting the formation and properties of clouds and thus radiative balance and
62 precipitation (Möhler et al., 2007; Ariya et al., 2009; Pratt et al., 2009; Pope, 2010; Pummer et al.,
63 2012; Gute and Abbatt, 2018). It has also been proposed that PBAPs may have significant impacts
64 on chemical composition of aerosol particles via heterogeneous and multiphase chemistry
65 (Deguillaume et al., 2008; Estillore et al., 2016; Reinmuth-Selzle et al., 2017; Shiraiwa et al., 2017).

66 Hygroscopicity is one of the most important physicochemical properties of pollen (as well
67 as aerosol particles in general). Hygroscopicity largely impacts the transport and deposition of
68 pollen grains (Sofiev et al., 2006), therefore affecting their lifetimes, abundance and

69 spatiotemporal distribution. In addition, hygroscopicity is closely linked to the ability of aerosol
70 particles to serve as CCN and INPs (Petters and Kreidenweis, 2007; Kreidenweis and Asa-Awuku,
71 2014; Laaksonen et al., 2016; Tang et al., 2016). Several previous studies have measured the
72 hygroscopicity and CCN activities of pollen (Diehl et al., 2001; Pope, 2010; Griffiths et al., 2012;
73 Lin et al., 2015; Steiner et al., 2015; Prisle et al., 2018) and other PBAPs such as bacteria (Pasanen
74 et al., 1991; Reponen et al., 1996; Franc and DeMott, 1998; Ko et al., 2000; Lee et al., 2002; Bauer
75 et al., 2003). For example, water uptake of eleven pollen species was studied using an analytical
76 balance (Diehl et al., 2001), and the mass of pollen was found to be increased by 3-16% at 73%
77 RH and by ~100-300% at 95% RH, compared to that at <1% RH. An electrodynamic balance was
78 employed to investigate hygroscopic growth of eight types of pollen (Pope, 2010; Griffiths et al.,
79 2012), and it was found that their hygroscopic growth can be approximated by the modified κ -
80 Köhler equation, with single hygroscopicity parameters being around 0.1 (depending on the
81 assumed pollen density, as discussed in Section 3.2).

82 Previous measurements were mostly carried out at or close to room temperature, and the
83 effects of temperature on hygroscopic properties of pollen and other types of PBAPs are yet to be
84 elucidated. To our knowledge, only one previous study (Bunderson and Levetin, 2015) explored
85 the effect of temperature (4, 15 and 20 °C) on water uptake by *Juniperus ashei*, *Juniperus*
86 *monosperma* and *Juniperus pinchotii* pollen. It is important to account for the temperature effects,
87 because ambient temperatures range from below -70 to >30 °C in the troposphere. In particular,
88 the altitude of 0.5-2.0 km to which pollen can be easily transported (Noh et al., 2013) may have
89 temperatures close to or lower than the chilling temperatures for vegetative species (up to 16.5 °C)
90 (Melke, 2015). Moreover, the temperature in the respiratory tract can reach up to 37 °C (the
91 physiological temperature). In the work presented here, a vapor sorption analyzer (VSA) was

92 employed to investigate hygroscopic growth of pollen grains at different temperature (5 or 15, 25,
93 and 37 °C), a range covering the chilling temperature to the physiological temperature. Water
94 uptake by pollen was also examined using diffusion reflectance infrared Fourier transform
95 spectroscopy at room temperature to complement the VSA results. Furthermore, transmission
96 Fourier transformation infrared spectroscopy was used to characterize functional groups of dry
97 pollen grains, in an attempt to seek potential links between chemical composition of pollen grains
98 and their hygroscopic properties.

99 **2 Experimental sections**

100 Six pollen species, all from anemophilous plants, were investigated in this work, including
101 populus tremuloides and populus deltoides (provided by Sigma Aldrich) as well as ragweed, corn,
102 pecan and paper mulberry (provided by Polysciences, Inc.). The six pollen species were chosen in
103 our work primarily because they were commercially available. Furthermore, these plants are also
104 widely distributed in the globe. For example, corn is the most produced grain in the world
105 (International-Grains-Council, 2019), and up to 50% of pollen-related allergic rhinitis cases in
106 North America are caused by ragweed pollen (Taramarcaz et al., 2005).

107 **2.1 Fourier transformation infrared spectroscopy**

108 The adsorption of water by pollen species were studied using in-situ diffusion reflectance
109 infrared Fourier transform spectroscopy (DRIFTS) at room temperature (~25 °C). This technique
110 was described in details in our previous work (Ma et al., 2010), and similar setups have also been
111 used by other groups to investigate adsorption of water by mineral dust (Joshi et al., 2017; Ibrahim
112 et al., 2018). Infrared spectra were recorded using a Nicolet 6700 Fourier transformation infrared
113 spectrometer (FTIR, Thermo Nicolet Instrument Corporation), equipped with an in-situ diffuse
114 reflection chamber and a high-sensitivity mercury cadmium telluride (MCT) detector cooled by

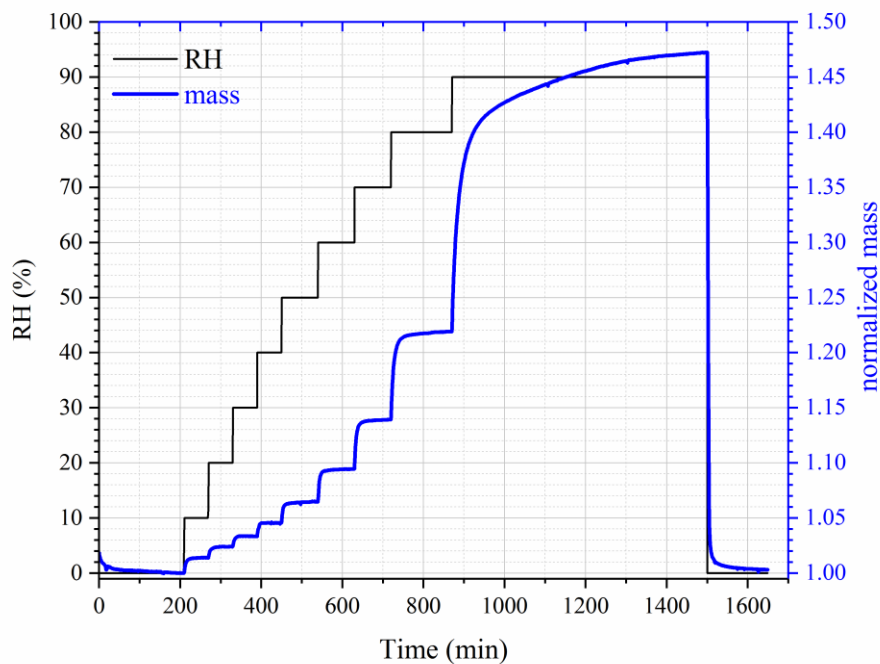
115 liquid nitrogen. A pollen sample (about 10 mg for each sample) under investigation was placed
116 into a ceramic crucible which was located in the in-situ chamber. A dry air flow and a humidified
117 air flow were first mixed and then delivered into the chamber, and the total flow rate was set to
118 200 mL/min (standard condition). Relative humidity (RH) in the chamber could be adjusted by
119 varying the flow rate ratio of the dry flow to the humidified flow, and was monitored online using
120 a moisture meter (CENTER 314) with an absolute uncertainty of $\pm 2\%$. Prior to each experiment,
121 the sample was flushed with dry air for 3 h at 25 °C, and the reference spectrum was recorded after
122 the pretreatment. Infrared spectra were collected and analyzed using OMNIC 6.0 software (Nicolet
123 Corp.). All the spectra reported here were recorded with a wavenumber resolution of 4 cm^{-1} , and
124 100 scans were averaged to produce a spectrum. Water adsorption was equilibrated for at least 30
125 min at each RH to ensure that the equilibrium between water vapor and adsorbed water was
126 reached.

127 Pollen samples used in this work were also characterized using transmission FTIR
128 equipped with a deuterated triglycine sulfate detector (DTGS) detector. Pollen grains and KBr
129 were mixed with a mass ratio of approximately 1:100 and ground in an agate mortar, and the
130 mixture was then pressed into a clear disc. Transmission FTIR was employed to examine these
131 discs, and a pure KBr disc was used as the reference. All the spectra, each of which was the average
132 of 100 scans, were also recorded with a wavenumber resolution of 4 cm^{-1} .

133 **2.2 Vapor sorption analyzer**

134 Hygroscopic growth of pollen grains was further investigated using a vapor sorption
135 analyzer (Q5000 SA, TA Instruments, New Castle, DE, USA) described in our previous work (Gu
136 et al., 2017; Guo et al., 2018; Jia et al., 2018). In brief, this instrument measured the sample mass
137 as a function of RH under isothermal conditions. The instrument can be operated in the temperature

138 range of 5-85 °C with a temperature accuracy of ± 0.1 °C and in the RH range of 0-98 % with an
139 absolute accuracy of $\pm 1\%$. RH in the humidity chamber was regulated by using two mass flow
140 controllers to control the dry and humidified nitrogen flows very precisely. The accuracy in RH
141 control was routinely checked by measuring the DRH values for a series of standard compounds,
142 e.g., NaCl, $(\text{NH}_4)_2\text{SO}_4$, KCl, and etc., and the difference between the measured and theoretical
143 DRH was always $< 1\%$. The mass measurement had a range of 0-100 mg and a sensitivity of ± 0.01
144 μg . The initial mass of each sample used in this work was in the range of 0.5-1 mg. For each of
145 the first three types of pollen species (populus tremuloides, populus deltoides and ragweed pollen),
146 three samples in total were investigated, and each sample was studied under isothermal conditions
147 at 5, 25 and 37 °C. For each of the other three types of pollen species (corn, pecan and paper
148 mulberry pollen), experiments were carried out at 15 °C instead of 5 °C, because the instrument
149 could only be cooled down to 15 °C due to a technical problem after we finished experiments for
150 the first three pollen species.



151

152 **Figure 1.** Change of RH (black curve, left y-axis) and normalized sample mass (blue curve, right
153 y-axis) with time for a typical experiment in which hygroscopic growth of pollen grains was
154 measured. In this figure a dataset for paper mulberry pollen at 25 °C is plotted as an example.
155

156 For the first sample, at each temperature the sample was first dried at 0% RH (the actual
157 RH was measured to be <1%); after that, RH was increased stepwise to 95% with an increment of
158 5% per step and then switched back to <1% to dry the sample again. At each RH, the sample was
159 equilibrated with the environment (i.e. until the sample mass became stable) before RH was
160 changed to the next value, and the sample mass was considered to be stabilized when the mass
161 change was <0.05% within 30 min. Such a measurement at one temperature could take several
162 days. In order to reduce experimental time, the second and third samples were investigated in a
163 similar way as the first sample, except that RH was increased stepwise to 90% with an increment
164 of 10% per step. A typical experimental dataset is displayed in Figure 1 as an example to illustrate
165 the change of RH and normalized sample mass with experimental time.

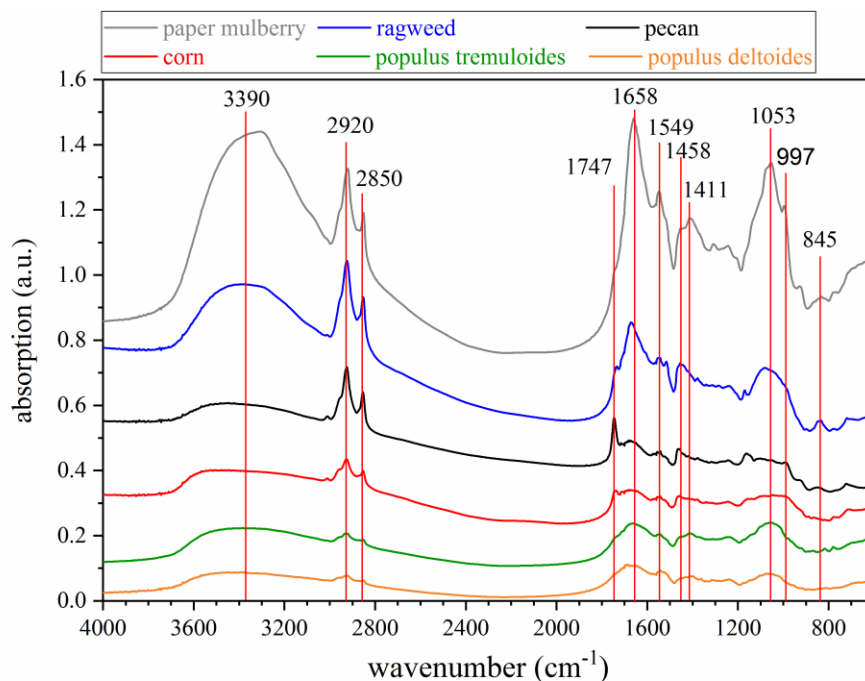
166 **3 Results and discussion**

167 **3.1 FTIR characterization of pollen samples**

168 **3.1.1 Infrared spectra of dry pollen samples**

169 Figure 2 shows the transmission FTIR spectra of the six pollen species investigated in our
170 work, and peak assignments can be found in Table 1. A broad band in the range of 3600-3000 cm^{-1} ,
171 attributed to O-H stretching vibration (Stuart, 2004; Pummer et al., 2013), and two sharp peaks at
172 2920 and 2850 cm^{-1} , attributed to C-H stretching (Eliason et al., 2003; Stuart, 2004; Pummer et al.,
173 2013), were observed for all the pollen species. The two peaks at 1747 and 1658 cm^{-1} were
174 assigned to alkyl ester carbonyls (Pappas et al., 2003; Najera et al., 2009; Pummer et al., 2013),

175 and the two peaks at 1549 and 1458 cm^{-1} (1411 cm^{-1} for paper mulberry pollen) were assigned to
176 C=C stretching and H-C-H deformation (Stuart, 2004; Pummer et al., 2013). In addition, the three
177 peaks at 1053, 997 and 845 cm^{-1} were assigned to C-O stretching, C-C stretching, and C-H out-of-
178 plane bending, respectively (Stuart, 2004; Najera et al., 2009; Pummer et al., 2013).



179
180 **Figure 2.** Transmission FTIR spectra of six pollen species investigated in this work.

181
182 OH groups and C-H groups in organic compounds are generally considered to be
183 hydrophilic and hydrophobic, and one may expect that the amount of OH groups (relative to that
184 of C-H groups) that organic samples contain may affect their hygroscopicity. For example, it was
185 found in many previous studies (Eliason et al., 2003; Asad et al., 2004; Hung et al., 2005; Najera
186 et al., 2009) that heterogeneous reactions of organic materials with O_3 and OH radicals would
187 increase the IR absorption intensity for the O-H stretching mode and decrease the IR absorption
188 intensity for the C-H stretching mode, meanwhile leading to the enhancement in their
189 hygroscopicity. Therefore, in this work we use the intensity ratio of the O-H stretching vibration

190 band (3000-3600 cm^{-1}) to the C-H stretching mode (2920 cm^{-1}) to qualitatively represent the
 191 amount of OH groups pollen samples contain. As shown in Figure 2, the six pollen species
 192 examined in our work can be roughly classified into two catalogues: 1) for populus deltoides,
 193 populus tremuloides and paper mulberry pollen, the O-H stretching vibration band is more
 194 intensive than the C-H stretching mode, indicating that they contain relatively high levels of OH
 195 groups; 2) for ragweed, pecan and corn pollen, the O-H stretching vibration band is less intensive
 196 than the C-H stretching mode, indicating that they contain relatively low levels of OH groups. The
 197 relation between the amount of OH groups that pollen species contain and their hygroscopicity
 198 will be further discussed in Section 3.3.

199

200 **Table 1.** Vibrational mode assignment for six pollen species investigated in this work.

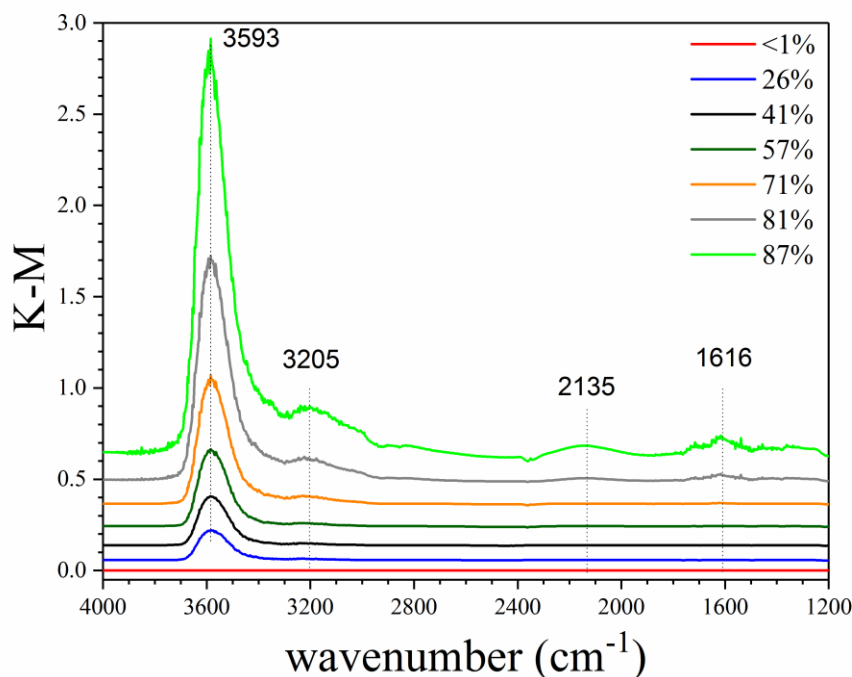
wavenumber (cm^{-1})	vibrational mode
3600-3000	O-H stretching
2920 and 2820	C-H stretching
1747 and 1658	alkyl ester carbonyls
1549	C=C stretching
1458 and 1411	H-C-H deformation
1053	C-O stretching
997	C-C stretching
845	C-H out-of-plane bending

201

202 3.1.2 Infrared spectra of pollen samples at different RH

203 In-situ DRIFTS was employed to explore adsorption of water by pollen grains. Typical
 204 spectra of populus deltoides pollen as a function of RH up to 87%, relative to that at <1% RH,
 205 are displayed in Figure 3. DRIFTS spectra of other pollen samples at different RH can be found in
 206 Figures S1-S5 in the supplement, and are very similar to those for populus deltoides pollen. As

207 evident from Figure 3, several IR peaks (e.g., 3593, 3205, 2135, and 1616 cm^{-1}) appeared in the
 208 spectra at elevated RH, when compared with that at <1% RH, and their intensities increased with
 209 increasing RH. The peaks at 3205, 2135 and 1616 cm^{-1} can be assigned to the stretching,
 210 association and bending modes of adsorbed water (Goodman et al., 2001; Schuttlefield et al.,
 211 2007a; Ma et al., 2010; Hatch et al., 2011; Song and Boily, 2013; Yeşilbaş and Boily, 2016; Joshi
 212 et al., 2017; Ibrahim et al., 2018).



213
 214 **Figure 3.** In-situ DRIFTS spectra of populus deltoides pollen as a function of RH (<1, 26, 41, 57,
 215 71, 81 and 87%) at 25 °C.

216
 217 The peak at $\sim 3600 \text{ cm}^{-1}$ was the most intensive one observed in the spectra, as shown in
 218 Figure 3. For comparison, the IR peaks assigned to the stretching mode of adsorbed water on
 219 mineral dust and NaCl appeared at lower wavenumbers, typically at around or lower than 3400
 220 cm^{-1} (Schuttlefield et al., 2007a; Ma et al., 2010; Tang et al., 2016; Ibrahim et al., 2018). As a
 221 result, the peak at $\sim 3600 \text{ cm}^{-1}$ may be assigned to the asymmetric stretching mode of water which

222 interacted with OH groups in pollen samples (Iwamoto et al., 2003). These results imply that water
 223 adsorption by pollen samples could be mainly contributed by OH groups of organic compounds
 224 they contained. Both C-OH and C(O)-OH groups can contribute to water adsorption by pollen
 225 samples, though their relative contribution cannot be resolved in our work. In addition, other
 226 factors, such as porosity and internal structure, may also be important for hygroscopic properties
 227 of pollen grains. The intensities of IR peaks at $\sim 3600\text{ cm}^{-1}$ were used to represent the amount of
 228 water adsorbed by pollen samples. Table 2 summarizes integrated areas of IR peaks at 3600 cm^{-1}
 229 as a function of RH for the six pollen species examined in our work, suggesting that the amount
 230 of adsorbed water by pollen samples increased with RH.

231
 232 **Table 2.** Integrated areas of IR peaks (at $\sim 3600\text{ cm}^{-1}$) of adsorbed water as a function of RH for
 233 the six pollen species investigated in this work. Wavenumber ranges used for integration are 3750-
 234 3300 cm^{-1} for populus deltoides pollen, 3750-3350 cm^{-1} for populus tremuloides pollen, 3750-
 235 3400 cm^{-1} for ragweed pollen, 3750-3500 cm^{-1} for corn pollen, 3750-3450 cm^{-1} for pecan pollen,
 236 and 3750-3300 cm^{-1} for paper mulberry pollen.

RH (%)	peak area	RH (%)	peak area	RH (%)	peak area
populus deltoides		populus tremuloides		ragweed	
<1	0	<1	0	<1	0
26	22.7	24	5.5	26	10.1
41	36.9	41	16.4	42	18.9
57	57.4	56	35.4	50	24.5
71	93.6	70	66.5	56	30.2
79	137.6	78	91.2	69	49.7
81	164.7	87	156.9	88	104.6
87	293.1				
corn		pecan		paper mulberry	
<1	0	<1	0	<1	0

26	10.0	26	8.6	26	10.2
42	21.5	43	16.9	43	17.7
58	41.9	58	29.5	51	23.1
73	87.5	73	60.0	59	29.8
89	222.2	89	338.9	71	46.7
				86	105.1

237

238 **3.2 Mass hygroscopic growth**

239 **3.2.1 Hygroscopicity parameterizations**

240 The single hygroscopicity parameter, κ , is widely used to describe the hygroscopicity of
 241 aerosol particles under both subsaturation and supersaturation (Petters and Kreidenweis, 2007).
 242 When the Kelvin effect is negligible (this is valid for pollen grains which are typically $>1 \mu\text{m}$), the
 243 dependence of diameter-based growth factor (GF) on RH can be linked to κ via Eq. (1) (Petters
 244 and Kreidenweis, 2007; Tang et al., 2016):

$$245 \quad RH = \frac{GF^3 - 1}{GF^3 - 1 + \kappa} \quad (1)$$

246 If we further assume that the particle is spherical, Eq. (1) can be transformed to Eq. (2):

$$247 \quad \frac{1}{RH} = 1 + \frac{\kappa}{GF^3 - 1} = 1 + \frac{\kappa}{\frac{V}{V_0} - 1} = 1 + \kappa \frac{V_0}{V - V_0} = 1 + \kappa \frac{V_0}{V_w} \quad (2)$$

248 where V , V_0 and V_w are the volumes of the particle at the given RH, the dry particle and water
 249 associated with the particle at the given RH. In order for Eq. (2) to be valid, it is also assumed that
 250 at a given RH, V is equal to the sum of V_0 and V_w . Eq. (2) can be further transformed to Eqs. (3-4):

$$251 \quad \frac{1}{RH} = 1 + \kappa \frac{\rho_w}{\rho_p} \frac{m_0}{m_w} \quad (3)$$

$$252 \quad \frac{m_w}{m_0} = \kappa \cdot \frac{\rho_w}{\rho_p} / \left(\frac{1}{RH} - 1 \right) \quad (4)$$

253 where ρ_w and ρ_p are the density of water and the dry particle, and m_0 and m_w are the mass of the
254 dry particle and water associated with the particle at the given RH. Since the particle mass, m , is
255 equal to the sum of m_0 and m_w , Eq. (5) can be derived from Eq. (4):

$$256 \quad \frac{m}{m_0} = 1 + \kappa \frac{\rho_w}{\rho_p} / \left(\frac{1}{RH} - 1 \right) \quad (5)$$

257 Using an electrodynamic balance, Pope and co-workers (Pope, 2010; Griffiths et al., 2012)
258 measured hygroscopic growth of eight types of pollen grains, and found that their mass change
259 with RH can be approximated by Eq. (5). It should be noted that the original equation derived by
260 Pope and co-workers (Pope, 2010; Griffiths et al., 2012) has a different format from but is
261 essentially equivalent to Eq. (5). Eq. (5) relates mass growth experimentally measured in our work
262 to the single hygroscopicity parameter (κ), which has been widely used in atmospheric science to
263 describe hygroscopic properties of aerosol particles under subsaturation as well as their CCN
264 activities under supersaturation; nevertheless, a few assumptions are needed to derive Eq. (5), as
265 discussed.

266 The Freundlich adsorption isotherm is another widely used equation to describe the change
267 of sample mass with RH due to water uptake (Atkins, 1998; Skopp, 2009; Hatch et al., 2011; Tang
268 et al., 2016):

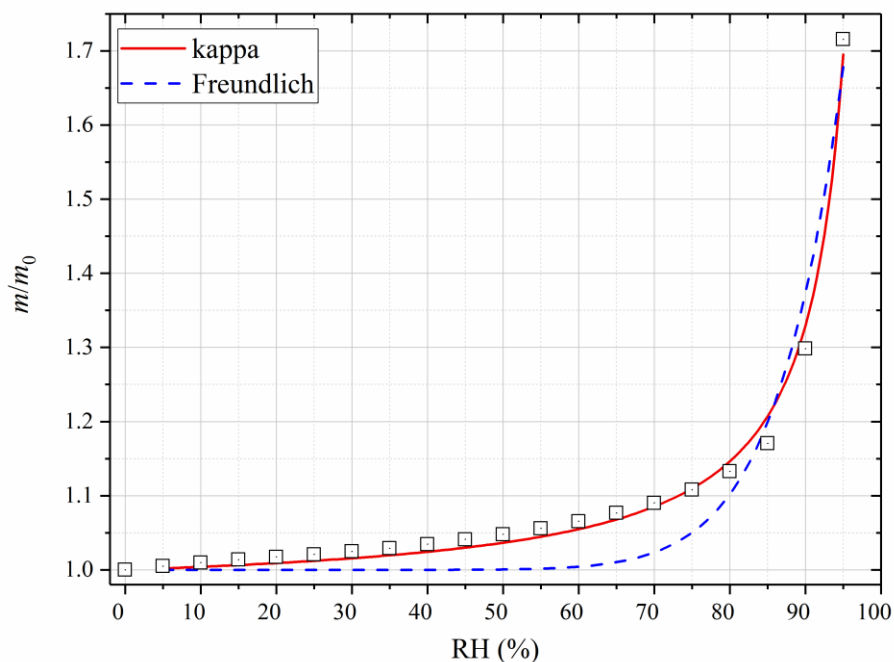
$$269 \quad \frac{m}{m_0} = 1 + A_f \cdot \sqrt[B_f]{RH} \quad (6)$$

270 where A_f and B_f are empirical Freundlich constants related to the adsorption capacity and strength.
271 One advantage of the Freundlich adsorption isotherm is that it provides a direct relationship
272 between RH and mass growth which was experimentally measured in our work, without any
273 additional assumptions. In addition, the BET (Brunauer-Emmett-Teller) adsorption isotherm is
274 also widely used to describe water adsorption by insoluble solid particles (Brunauer et al., 1938;
275 Goodman et al., 2001; Henson, 2007; Ma et al., 2010; Tang et al., 2016; Joshi et al., 2017). While

276 the BET adsorption isotherm typically works well for water adsorption of a few monolayers, the
277 mass of adsorbed water, as shown in Section 3.2.2, can reach up to 50% of the dry pollen mass at
278 high RH; therefore, in this work we did not attempt to use the BET adsorption isotherm to describe
279 water adsorption by pollen grains. Another reason that we did not attempt to use the BET
280 adsorption isotherm is that the BET adsorption isotherm is mathematically more complex and
281 requires the BET surface area to be known.

282 3.2.2 Mass hygroscopic growth at room temperature

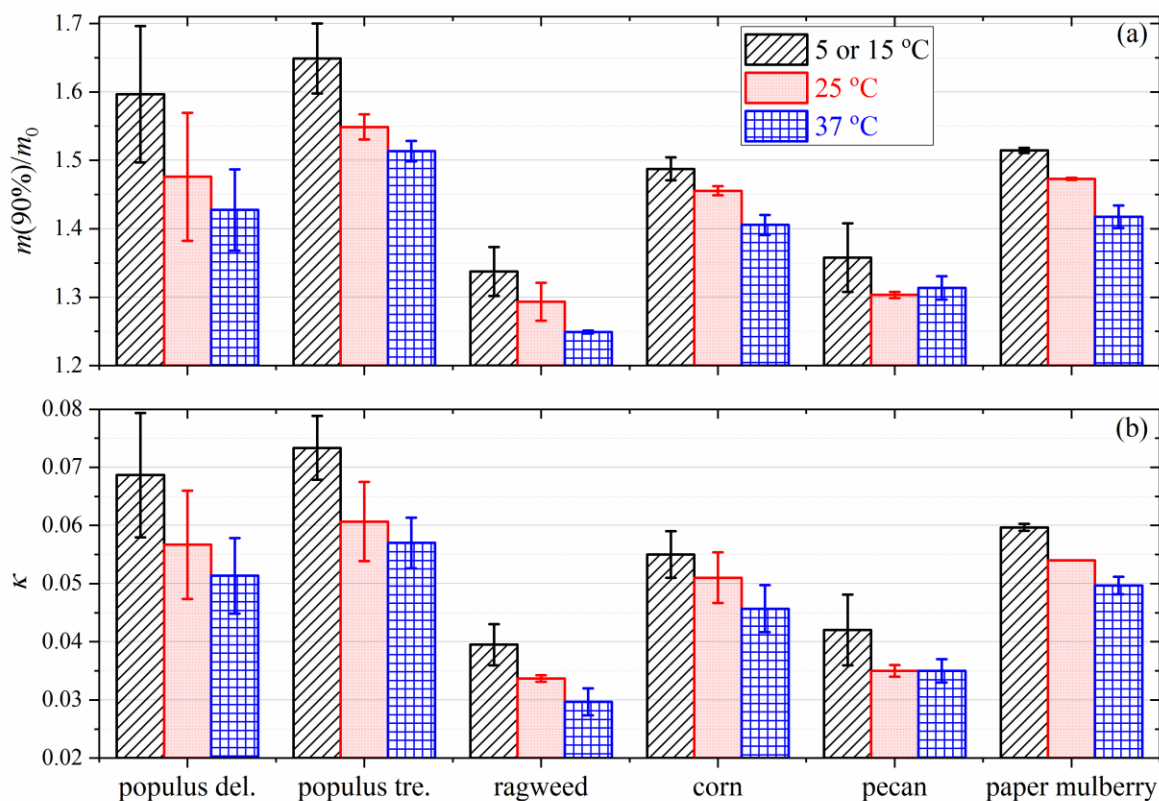
283 Figure 4 displays the sample mass (normalized to that at 0% RH) as a function of RH for
284 pecan pollen at 25 °C. Significant increase in sample mass was observed at elevated RH due to
285 uptake of water. Compared to that at <1% RH, the sample mass increased by (2.3±0.3)% at 30%
286 RH, (6.4±0.2)% at 60% RH, (30.3±0.4)% at 90% RH, and up to ~72% at 95% RH. As shown by
287 the data compiled in Tables S1-S3 in the supplement, substantial increases in sample mass were
288 also observed for the other five types of pollen species at 25 °C (as well as 5 and 37 °C).



289

290 **Figure 4.** Measured change of sample mass (normalized to that at dry conditions, i.e. m/m_0) of
291 pecan pollen as a function of RH (0-95%) at 25 °C. The experimental data are fitted with the
292 modified κ -Köhler equation (solid red curve) and the Freundlich adsorption isotherm (dashed blue
293 curve).

294
295 Hygroscopic properties exhibited considerable variations among different pollen species.
296 Figure 5a compares the measured ratios of sample mass at 90% RH to that at <1% RH, $m(90\%)/m_0$,
297 for the six pollen species investigated in this work. We specifically discuss mass changes of pollen
298 grains at 90% RH (relative to that at <1% RH) because aerosol hygroscopic growth at 90% RH
299 was widely reported by laboratory and field studies (Kreidenweis and Asa-Awuku, 2014). As
300 shown in Figure 5a, $m(90\%)/m_0$ determined at 25 °C ranged from 1.293 ± 0.028 (ragweed pollen)
301 to 1.476 ± 0.094 (populus deltoides pollen), i.e. the amount of water adsorbed/absorbed by the six
302 different pollen species at 90% RH varied between ~30% to ~50% of the dry mass.



303
 304 **Figure 5.** Measured ratios of sample mass at 90% RH to that at <1% RH (a) and derived κ values
 305 (b) for six pollen species at different temperatures. The lowest temperatures were 5 °C for populus
 306 deltoides (populus del.), populus tremuloides (populus tre.) and ragweed pollen, and 15 °C for corn,
 307 pecan and paper mulberry pollen.

308
 309 As shown in Figure 4, the increase of pecan pollen mass with RH at 25 °C could be
 310 satisfactorily described by the modified κ -Köhler equation for the entire RH range (up to 95%).
 311 On the contrary, the Freundlich adsorption isotherm significantly underestimated the sample mass
 312 at low RH, although it represented the experimental data at high RH reasonably well. In addition,
 313 we found that the modified κ -Köhler equation could also approximate the dependence of sample
 314 mass on RH for all the six types of pollen species investigated in this work at different temperatures.

315 If we use Eq. (5) to fit m/m_0 against RH, $\kappa \cdot \rho_w/\rho_p$ can be derived. The bulk densities of dry pollen
 316 grains were found to vary with species but typically fall into the range of 0.5-2 g cm⁻³ (Harrington
 317 and Metzger, 1963; Hirose and Osada, 2016), and for simplicity ρ_p was assumed to be 1 g cm⁻³ in
 318 this work (i.e. ρ_w/ρ_p is equal to 1). With the assumptions on dry particle density and also particle
 319 sphericity, κ could then be derived from the measured RH-dependent sample mass at a given
 320 temperature.

321 Table 3 summarizes the average κ values at different temperatures for the six pollen species
 322 investigated in this work. At 25 °C, the κ values were found to increase from 0.034±0.001 for
 323 ragweed pollen to 0.061±0.007 for populus tremuloides pollen, varied by almost a factor of 2. The
 324 κ values measured by Pope and co-workers (Pope, 2010; Griffiths et al., 2012) were approximately
 325 in the range of 0.05-0.11 (assuming that ρ_w/ρ_p is equal to 1), in reasonably good agreement with
 326 these reported in our work. It should be noted that in order to convert the measured mass growth
 327 to diameter growth and κ values, one key assumption is particle sphericity; nevertheless, pollen
 328 grains are known to be non-spherical and porous, and therefore our derived κ values might be
 329 smaller than the actual values. For example, although the mass increase was substantial (around
 330 30-50 % at 90% RH) for the six pollen species examined, their κ values at 25 °C were derived to
 331 be in the range of 0.034-0.061, significantly smaller than those (0.1-0.2) for typical secondary
 332 organic aerosols produced in smog chamber studies (Petters and Kreidenweis, 2007; Kreidenweis
 333 and Asa-Awuku, 2014).

334
 335 **Table 3.** Single hygroscopicity parameters (κ) derived in this work for the six pollen species at
 336 different temperatures. All the errors given in this work are standard deviations.

pollen type	T (°C)	sample 1	sample 2	sample 3	average
	5	0.071±0.001	0.078±0.001	0.057±0.002	0.069±0.011

populus	25	0.054±0.001	0.067±0.002	0.049±0.002	0.057±0.009
deltoides	37	0.058±0.002	0.051±0.001	0.045±0.002	0.051±0.007
populus	5	0.068±0.001	0.073±0.001	0.079±0.001	0.073±0.006
tremuloides	25	0.053±0.002	0.063±0.002	0.066±0.002	0.061±0.007
	37	0.052±0.002	0.059±0.002	0.060±0.002	0.057±0.004
ragweed	5	0.042±0.001	0.037±0.002	--	0.040±0.004
	25	0.033±0.002	0.034±0.003	0.034±0.002	0.034±0.001
	37	0.027±0.001	0.031±0.002	0.031±0.002	0.030±0.002
corn	15	0.051±0.001	0.059±0.002	0.055±0.002	0.055±0.004
	25	0.046±0.002	0.053±0.002	0.054±0.002	0.051±0.004
	37	0.041±0.002	0.048±0.002	0.048±0.002	0.046±0.004
pecan	15	0.049±0.001	0.038±0.001	0.039±0.001	0.042±0.006
	25	0.036±0.001	0.034±0.001	0.035±0.001	0.035±0.001
	37	0.033±0.001	0.035±0.002	0.037±0.001	0.035±0.002
paper	15	0.059±0.002	0.060±0.002	0.060±0.002	0.060±0.001
mulberry	25	0.054±0.001	0.054±0.001	0.054±0.001	0.054±0.001
	37	0.048±0.002	0.050±0.002	0.051±0.002	0.050±0.002

337

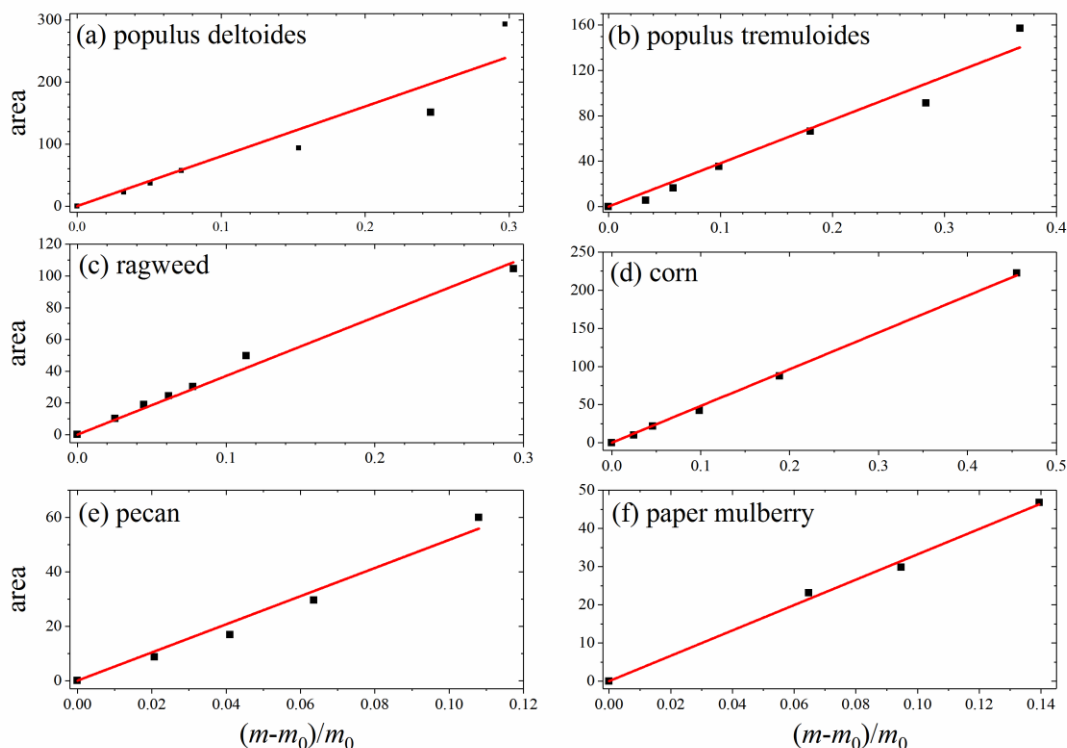
338 **3.3 Discussion**

339 **3.3.1 Reconciliation between IR and VSA results**

340 Our in-situ DRIFTS measurements, as discussed in Section 3.1.2, suggested that water
341 uptake by pollen samples was mainly contributed by OH groups of organic compounds they
342 contained; therefore, one may expect that pollen species which contain higher levels of OH groups
343 would exhibit higher hygroscopicity. Transmission FTIR characterization of pollen species
344 (Section 3.1.1) showed that populus deltoides, populus tremuloides and paper mulberry pollen
345 contained relatively high levels of OH groups, and indeed their hygroscopicity (κ : 0.053-0.054 at
346 25 °C) was higher than the other three pollen species, as shown in Figure 5 and Table 3. For
347 comparison, ragweed and pecan pollen contained relatively low levels of OH groups and
348 correspondingly exhibited lower hygroscopicity (κ : 0.033-0.036 at 25 °C). Corn pollen appeared

349 to be an exception: it contained relatively low levels of OH groups but displayed medium
350 hygroscopicity (κ : ~ 0.046 at $25\text{ }^\circ\text{C}$). As a result, our results may imply that in addition to chemical
351 composition, other physicochemical properties, such as porosity and internal structure of pollen
352 grains, could also play an important role in determining the hygroscopicity of pollen species. One
353 clue came from environmental scanning electron microscopy observations (Pope, 2010), revealing
354 that pollen grains started to swell internally before significant water uptake on the surface took
355 place.

356 In our work two complementary techniques were employed to explore hygroscopic
357 properties of pollen species. VSA measured the amount of water absorbed/adsorbed by pollen
358 grains as a function of RH in a quantitative manner, whereas the intensities of IR peaks of adsorbed
359 water at different RH, as characterized by DRIFTS, can be used semi-quantitatively to represent
360 the amount of water associated with particles (Goodman et al., 2001; Schuttlefield et al., 2007b;
361 Ma et al., 2010; Yeşilbaş and Boily, 2016; Joshi et al., 2017; Ibrahim et al., 2018). We compare
362 our VSA results (i.e. the relative mass change due to water uptake) to the DRIFTS results (i.e.
363 integrated area of IR peaks at $\sim 3600\text{ cm}^{-1}$). As shown in Figure 6, good correlations between VSA
364 and DRIFTS results are found for all the six pollen species, suggesting that DRIFTS can be used
365 to represent the amount of adsorbed water, at least in a semi-quantitative manner.



366
 367 **Figure 6.** Integrated areas of IR peaks at $\sim 3600\text{ cm}^{-1}$ versus relative mass increase due to water
 368 uptake, $(m-m_0)/m_0$, for six pollen species: (a) populus deltoides; (b) populus tremuloides; (c)
 369 ragweed; (d) corn; (e) pecan; (f) paper mulberry.

370
 371 **3.3.2 Effect of temperature**

372 Figure 5a shows the comparison of the measured ratios of sample mass at 90% RH to that
 373 at $<1\%$ RH, $m(90\%)/m_0$, at different temperatures for the six pollen species. It can be concluded
 374 from Figure 5a that except for pecan pollen for which a small increase in $m(90\%)/m_0$ occurred
 375 when temperature increased from 25 to 37 °C, increase in temperature would lead to small but
 376 nevertheless significant decrease in $m(90\%)/m_0$. For example, $m(90\%)/m_0$ decreased from
 377 1.597 ± 0.100 at 5 °C to 1.476 ± 0.094 at 25 °C and to 1.427 ± 0.060 at 37 °C for populus deltoides

378 pollen, and from 1.338 ± 0.036 at 5 °C to 1.293 ± 0.028 at 25 °C and to 1.249 ± 0.002 at 37 °C for
379 ragweed pollen.

380 We further derived κ values at different temperatures for the six pollen species, and the
381 results are plotted in Figure 5b and summarized in Table 3. Increase in temperature would lead to
382 decrease in κ values, except for pecan pollen. For example, κ decreased from 0.073 ± 0.006 at 5 °C
383 to 0.057 ± 0.004 at 37 °C for populus tremuloides pollen, and decreased from 0.060 ± 0.001 at 15 °C
384 to 0.050 ± 0.002 at 37 °C for paper mulberry pollen.

385 **4 Conclusion and implications**

386 Pollen grains are one of the most abundant types of primary biological aerosol particles in
387 the troposphere and play important roles in many aspects of the Earth system. Hygroscopicity is
388 among the most important physicochemical properties of pollen grains and largely affect their
389 environmental, health and climatic impacts. However, our knowledge in their hygroscopicity is
390 still quite limited, and especially the temperature effect has been rarely explored.

391 In this work we investigated hygroscopic properties of six types of pollen species as a
392 function of RH (up to 95%) at 5 (or 15), 25 and 37 °C. Substantial increase in pollen mass was
393 observed at elevated RH due to water uptake for all the six pollen species. Therefore, change in
394 the mass of pollen grains and their aerodynamic properties at different RH should be taken into
395 account to better understand their transport and deposition in the troposphere. It was found that the
396 mass hygroscopic growth of pollen grains can be well approximated by the modified κ -Köhler
397 equation. The derived κ values at 25 °C ranged from 0.034 ± 0.001 to 0.061 ± 0.007 , varying with
398 pollen species. DRIFTS measurements indicated that water adsorption by pollen species were
399 mainly contributed by OH groups of organic compounds contained by pollen grains, and indeed
400 pollen species that contained lower levels of OH groups (relative to C-H groups, as determined

401 using transmission FTIR) showed lower hygroscopicity. One exception was corn pollen which
402 contained low levels of OH group but exhibited medium hygroscopicity, suggesting that in
403 addition to chemical composition, other physicochemical properties, such as porosity and internal
404 structure, might also play an important role in determining the hygroscopicity of pollen grains.
405 Due to their moderate hygroscopicity as well as large sizes, pollen grains can thus act as efficient
406 giant CCN which may have significant impacts on cloud and precipitation (Johnson, 1982;
407 Feingold et al., 1999; Yin et al., 2000; Posselt and Lohmann, 2008). It is worth noting that only
408 six different pollen species were examined in our work, and hygroscopic properties of other pollen
409 species commonly found in the troposphere should be further investigated.

410 The effect of temperature on the hygroscopicity of pollen grains was systematically
411 investigated in this work. Increase in temperature (from 5 or 15 °C to 25 and 37 °C), a range
412 covering chilling temperature to physiological temperature, led to small but detectable decrease in
413 pollen hygroscopicity. For example, κ values were found to decrease from 0.073 ± 0.006 at 5 °C to
414 0.061 ± 0.007 at 25 °C and to 0.057 ± 0.004 at 37 °C for populus tremuloides pollen, and decrease
415 from 0.060 ± 0.001 at 15 °C to 0.054 ± 0.001 at 25 °C to 0.050 ± 0.002 at 37 °C for paper mulberry
416 pollen. Our measurements at 37 °C (physiological temperature) provide very valuable parameters
417 which can be used in numerical models to better understand the transport and deposition of pollen
418 particles in the respiratory system and thus their impacts on human health (Yeh et al., 1996; Broday
419 and Georgopoulos, 2001; Park and Wexler, 2008; Lambert et al., 2011; Longest and Holbrook,
420 2012; Tong et al., 2014). Nevertheless, it should be noted that due to the short residence time in
421 the respiratory system, pollen grains and other inhaled particles in general, may not reach
422 equilibrium with water vapor in the respiratory tract.

423 Due to technical challenges, the lowest temperature we could reach in this work was 5 °C,
424 in the range of normal chilling temperatures for vegetative species and also in the expected
425 temperature range at the altitudes of 0.5-2.0 km to which pollen grains can be easily transported.
426 Temperatures in the upper troposphere can be as low as below -70 °C, and it is yet to be explored
427 whether further decrease in temperature to far below 0 °C will lead to large increase in pollen
428 hygroscopicity. As a result, experimental measurements of pollen hygroscopicity at lower
429 temperatures are warranted and would significantly help better understand the transport of pollen
430 grains in the troposphere. Since water vapor has to be adsorbed or condensed on ice nucleating
431 particles before heterogeneous ice nucleation can take place (Laaksonen et al., 2016), knowledge
432 in hygroscopicity and water uptake at temperatures below 0 °C would provide fundamental insights
433 into atmospheric ice nucleation, in which pollen grains may play an important role (Pratt et al.,
434 2009; Prenni et al., 2009; Hoose et al., 2010; Pöschl et al., 2010; Murray et al., 2012; Creamean et
435 al., 2013; Tang et al., 2018).

436

437 **Data availability.** All the data are available from Mingjin Tang (mingjintang@gig.ac.cn) up on
438 request.

439 **Competing interests.** The authors declare that they have no conflict of interest.

440 **Author contribution.** MT, QM and YJL designed the research; WG, CZ, SL and XY did the
441 measurements; MT, QM, YJL and RJH analyzed the results; MT, QM, YJL and RJH wrote the
442 manuscript with contribution from all the co-authors.

443 **Acknowledgment.** This work was funded by National Natural Science Foundation of China
444 (91644106, 91744204 and 91644219), Chinese Academy of Sciences (132744KYSB20160036),
445 Science and Technology Development Fund of Macau (016/2017/A1), and State Key Laboratory

446 of Organic Geochemistry (SKLOG2016-A05). Mingjin Tang would like to thank the CAS Pioneer
447 Hundred Talents program for providing a starting grant. **This is contribution No.IS-XXXX from**
448 **GIGCAS.**

449 **Reference**

- 450 Ariya, P. A., Sun, J., Eltouny, N. A., Hudson, E. D., Hayes, C. T., and Kos, G.: Physical and chemical
451 characterization of bioaerosols – Implications for nucleation processes, *Int. Rev. Phys. Chem.*, 28, 1-32, 2009.
- 452 Asad, A., Mmereki, B. T., and Donaldson, D. J.: Enhanced uptake of water by oxidatively processed oleic acid,
453 *Atmos. Chem. Phys.*, 4, 2083-2089, 2004.
- 454 Atkins, P. W.: *Physical Chemistry (Sixth Edition)*, Oxford University Press, Oxford, UK, 1998.
- 455 Bauer, H., Giebl, H., Hitznerberger, R., Kasper-Giebl, A., Reischl, G., Zibuschka, F., and Puxbaum, H.: Airborne
456 bacteria as cloud condensation nuclei, *J. Geophys. Res.-Atmos.*, 108, 4658, doi: 4610.1029/2003JD003545, 2003.
- 457 Broday, D. M., and Georgopoulos, P. G.: Growth and Deposition of Hygroscopic Particulate Matter in the Human
458 Lungs, *Aerosol Sci. Technol.*, 34, 144-159, 2001.
- 459 Brunauer, S., Emmett, P. H., and Teller, E.: Adsorption of Gases in Multimolecular Layers, *J. Am. Chem. Soc.*, 60,
460 309-319, 1938.
- 461 Bunderson, L. D., and Levetin, E.: Hygroscopic weight gain of pollen grains from *Juniperus* species, *Int. J.*
462 *Biometeorol.*, 59, 533-540, 2015.
- 463 Creamean, J. M., Suski, K. J., Rosenfeld, D., Cazorla, A., DeMott, P. J., Sullivan, R. C., White, A. B., Ralph, F. M.,
464 Minnis, P., Comstock, J. M., Tomlinson, J. M., and Prather, K. A.: Dust and Biological Aerosols from the Sahara
465 and Asia Influence Precipitation in the Western U.S, *Science*, 339, 1572-1578, 2013.
- 466 Deguillaume, L., Leriche, M., Amato, P., Ariya, P. A., Delort, A. M., Poschl, U., Chaumerliac, N., Bauer, H.,
467 Flossmann, A. I., and Morris, C. E.: Microbiology and atmospheric processes: chemical interactions of primary
468 biological aerosols, *Biogeosciences*, 5, 1073-1084, 2008.
- 469 Després, V. R., Huffman, J. A., Burrows, S. M., Hoose, C., Safatov, A. S., Buryak, G., Fröhlich-Nowoisky, J.,
470 Elbert, W., Andreae, M. O., Pöschl, U., and Jaenicke, R.: Primary biological aerosol particles in the atmosphere: a
471 review, *Tellus B*, 64, 15598, 2012.
- 472 Diehl, K., Quick, C., Matthias-Maser, S., Mitra, S. K., and Jaenicke, R.: The ice nucleating ability of pollen - Part I:
473 Laboratory studies in deposition and condensation freezing modes, *Atmos. Res.*, 58, 75-87, 2001.
- 474 Douwes, J., Thorne, P., Pearce, N., and Heederik, D.: Bioaerosol health effects and exposure assessment: Progress
475 and prospects, *Ann. Occup. Hyg.*, 47, 187-200, 2003.
- 476 Eliason, T. L., Aloisio, S., Donaldson, D. J., Cziczo, D. J., and Vaida, V.: Processing of unsaturated organic acid
477 films and aerosols by ozone, *Atmos. Environ.*, 37, 2207-2219, 2003.
- 478 Estillore, A. D., Trueblood, J. V., and Grassian, V. H.: Atmospheric chemistry of bioaerosols: heterogeneous and
479 multiphase reactions with atmospheric oxidants and other trace gases, *Chem. Sci.*, 7, 6604-6616, 2016.
- 480 Feingold, G., Cotton, W. R., Kreidenweis, S. M., and Davis, J. T.: The Impact of Giant Cloud Condensation Nuclei
481 on Drizzle Formation in Stratocumulus: Implications for Cloud Radiative Properties, *J. Atmos. Sci.*, 56, 4100-4117,
482 1999.
- 483 Fröhlich-Nowoisky, J., Kampf, C. J., Weber, B., Huffman, J. A., Pöhlker, C., Andreae, M. O., Lang-Yona, N.,
484 Burrows, S. M., Gunthe, S. S., Elbert, W., Su, H., Hoor, P., Thines, E., Hoffmann, T., Després, V. R., and Pöschl,
485 U.: Bioaerosols in the Earth system: Climate, health, and ecosystem interactions, *Atmos. Res.*, 182, 346-376, 2016.
- 486 Franc, G. D., and DeMott, P. J.: Cloud activation characteristics of airborne *Erwinia carotovora* cells, *J. Appl. Met.*,
487 37, 1293-1300, 1998.
- 488 Georgakopoulos, D. G., Després, V., Fröhlich-Nowoisky, J., Psenner, R., Ariya, P. A., Pósfai, M., Ahern, H. E.,
489 Moffett, B. F., and Hill, T. C. J.: Microbiology and atmospheric processes: biological, physical and chemical
490 characterization of aerosol particles, *Biogeosciences*, 6, 721-737, 2009.
- 491 Goodman, A. L., Bernard, E. T., and Grassian, V. H.: Spectroscopic Study of Nitric Acid and Water Adsorption on
492 Oxide Particles: Enhanced Nitric Acid Uptake Kinetics in the Presence of Adsorbed Water, *J. Phys. Chem. A*, 105,
493 6443-6457, 2001.
- 494 Griffiths, P. T., Borlace, J. S., Gallimore, P. J., Kalberer, M., Herzog, M., and Pope, F. D.: Hygroscopic growth and
495 cloud activation of pollen: a laboratory and modelling study, *Atmos. Sci. Lett.*, 13, 289-295, 2012.

496 Gu, W. J., Li, Y. J., Zhu, J. X., Jia, X. H., Lin, Q. H., Zhang, G. H., Ding, X., Song, W., Bi, X. H., Wang, X. M., and
497 Tang, M. J.: Investigation of water adsorption and hygroscopicity of atmospherically relevant particles using
498 a commercial vapor sorption analyzer, *Atmos. Meas. Tech.*, 10, 3821-3832, 2017.

499 Guo, L. Y., Gu, W. J., Peng, C., Wang, W. G., Li, Y. J., Zong, T. M., Tang, Y. J., Wu, Z. J., Lin, Q. H., Ge, M. F.,
500 Zhang, G. H., Hu, M., Bi, X. H., Wang, X. M., and Tang, M. J.: A comprehensive study of hygroscopic properties of
501 calcium- and magnesium-containing salts: implication for hygroscopicity of mineral dust and sea salt aerosols,
502 *Atmos. Chem. Phys. Discuss.*, 2018, 1-37, 10.5194/acp-2018-412, 2018.

503 Gute, E., and Abbatt, J. P. D.: Oxidative Processing Lowers the Ice Nucleation Activity of Birch and Alder Pollen,
504 *Geophys. Res. Lett.*, 45, 1647-1653, 2018.

505 Harrington, J. B., and Metzger, K.: Ragweed Pollen Density, *Amer. J. Bot.*, 50, 532-539, 1963.

506 Hatch, C. D., Wiese, J. S., Crane, C. C., Harris, K. J., Kloss, H. G., and Baltrusaitis, J.: Water Adsorption on Clay
507 Minerals As a Function of Relative Humidity: Application of BET and Freundlich Adsorption Models, *Langmuir*,
508 28, 1790-1803, 2011.

509 Henson, B. F.: An adsorption model of insoluble particle activation: Application to black carbon, *J. Geophys. Res. -*
510 *Atmos.*, 112, D24S16, doi: 10.1029/2007JD008549, 2007.

511 Hirose, Y., and Osada, K.: Terminal settling velocity and physical properties of pollen grains in still air,
512 *Aerobiologia*, 32, 385-394, 2016.

513 Hoose, C., Kristjansson, J. E., and Burrows, S. M.: How important is biological ice nucleation in clouds on a global
514 scale?, *Environ. Res. Lett.*, 5, 024009, 2010.

515 Hung, H. M., Katrib, Y., and Martin, S. T.: Products and mechanisms of the reaction of oleic acid with ozone and
516 nitrate radical, *J. Phys. Chem. A*, 109, 4517-4530, 2005.

517 Ibrahim, S., Romanias, M. N., Alleman, L. Y., Zeineddine, M. N., Angeli, G. K., Trikalitis, P. N., and Thevenet, F.:
518 Water Interaction with Mineral Dust Aerosol: Particle Size and Hygroscopic Properties of Dust, *ACS Earth and*
519 *Space Chem.*, 2, 376-386, 2018.

520 International-Grains-Council: Grain Market Report GMR 495, 2019.

521 Iwamoto, R., Matsuda, T., Sasaki, T., and Kusanagi, H.: Basic interactions of water with organic compounds, *J.*
522 *Phys. Chem. B*, 107, 7976-7980, 2003.

523 Jia, X. H., Gu, W. J., Li, Y. J., Cheng, P., Tang, Y. J., Guo, L. Y., Wang, X. M., and Tang, M. J.: Phase transitions
524 and hygroscopic growth of Mg(ClO₄)₂, NaClO₄, and NaClO₄·H₂O: implications for the stability of aqueous water
525 in hyperarid environments on Mars and on Earth, *ACS Earth Space Chem.*, 2, 159-167, 2018.

526 Johnson, D. B.: The Role of Giant and Ultragiant Aerosol Particles in Warm Rain Initiation, *J. Atmos. Sci.*, 39, 448-
527 460, 1982.

528 Joshi, N., Romanias, M. N., Riffault, V., and Thevenet, F.: Investigating water adsorption onto natural mineral dust
529 particles: Linking DRIFTS experiments and BET theory, *Aeolian Res.*, 27, 35-45, 2017.

530 Ko, G., First, M. W., and Burge, H. A.: Influence of relative humidity on particle size and UV sensitivity of *Serratia*
531 *marcescens* and *Mycobacterium bovis* BCG aerosols, *Tubercle and Lung Disease*, 80, 217-228, 2000.

532 Kreidenweis, S. M., and Asa-Awuku, A.: 5.13 - Aerosol Hygroscopicity: Particle Water Content and Its Role in
533 Atmospheric Processes, in: *Treatise on Geochemistry (Second Edition)*, edited by: Turekian, K. K., Elsevier,
534 Oxford, 331-361, 2014.

535 Laaksonen, A., Malila, J., Nenes, A., Hung, H. M., and Chen, J. P.: Surface fractal dimension, water adsorption
536 efficiency, and cloud nucleation activity of insoluble aerosol, *Scientific Reports*, 6, 25504, doi:
537 25510.21038/srep25504, 2016.

538 Lambert, A. R., O'Shaughnessy, P. T., Tawhai, M. H., Hoffman, E. A., and Lin, C. L.: Regional Deposition of
539 Particles in an Image-Based Airway Model: Large-Eddy Simulation and Left-Right Lung Ventilation Asymmetry,
540 *Aerosol Sci. Technol.*, 45, 11-25, 2011.

541 Lee, B. U., Kim, S. H., and Kim, S. S.: Hygroscopic growth of *E. coli* and *B. subtilis* bioaerosols, *J. Aerosol. Sci.*, 33,
542 1721-1723, 2002.

543 Lin, H., Lizarraga, L., Bottomley, L. A., and Carson Meredith, J.: Effect of water absorption on pollen adhesion, *J.*
544 *Colloid Interface Sci.*, 442, 133-139, 2015.

545 Longest, P. W., and Holbrook, L. T.: In silico models of aerosol delivery to the respiratory tract - Development and
546 applications, *Advanced Drug Delivery Reviews*, 64, 296-311, 2012.

547 Möhler, O., DeMott, P. J., Vali, G., and Levin, Z.: Microbiology and atmospheric processes: the role of biological
548 particles in cloud physics, *Biogeosciences*, 4, 1059-1071, 2007.

549 Ma, Q. X., He, H., and Liu, Y. C.: In Situ DRIFTS Study of Hygroscopic Behavior of Mineral Aerosol, *J. Environ.*
550 *Sci.*, 22, 555-560, 2010.

551 Melke, A.: The Physiology of Chilling Temperature Requirements for Dormancy Release and Bud-break in
552 Temperate Fruit Trees Grown at Mild Winter Tropical Climate, *Journal of Plant Studies*, 4, 110-156, 2015.

553 Morris, C. E., Sands, D. C., Bardin, M., Jaenicke, R., Vogel, B., Leyronas, C., Ariya, P. A., and Psenner, R.:
554 Microbiology and atmospheric processes: research challenges concerning the impact of airborne micro-organisms
555 on the atmosphere and climate, *Biogeosciences*, 8, 17-25, 2011.

556 Morris, C. E., Conen, F., Alex Huffman, J., Phillips, V., Pöschl, U., and Sands, D. C.: Bioprecipitation: a feedback
557 cycle linking Earth history, ecosystem dynamics and land use through biological ice nucleators in the atmosphere,
558 *Glob. Chang. Biol.*, 20, 341-351, 2014.

559 Murray, B. J., O'Sullivan, D., Atkinson, J. D., and Webb, M. E.: Ice nucleation by particles immersed in supercooled
560 cloud droplets, *Chem. Soc. Rev.*, 41, 6519-6554, 2012.

561 Najera, J. J., Percival, C. J., and Horn, A. B.: Infrared spectroscopic studies of the heterogeneous reaction of ozone
562 with dry maleic and fumaric acid aerosol particles, *Physical Chemistry Chemical Physics*, 11, 9093-9103, 2009.

563 Noh, Y. M., Lee, H., Mueller, D., Lee, K., Shin, D., Shin, S., Choi, T. J., Choi, Y. J., and Kim, K. R.: Investigation
564 of the diurnal pattern of the vertical distribution of pollen in the lower troposphere using LIDAR, *Atmos. Chem.*
565 *Phys.*, 13, 7619-7629, 2013.

566 Pöschl, U., Martin, S. T., Sinha, B., Chen, Q., Gunthe, S. S., Huffman, J. A., Borrmann, S., Farmer, D. K., Garland,
567 R. M., Helas, G., Jimenez, J. L., King, S. M., Manzi, A., Mikhailov, E., Pauliquevis, T., Petters, M. D., Prenni, A. J.,
568 Roldin, P., Rose, D., Schneider, J., Su, H., Zorn, S. R., Artaxo, P., and Andreae, M. O.: Rainforest Aerosols as
569 Biogenic Nuclei of Clouds and Precipitation in the Amazon, *Science*, 329, 1513-1516, 2010.

570 Pappas, C. S., Tarantilis, P. A., Harizanis, P. C., and Polissiou, M. G.: New method for pollen identification by FT-
571 IR spectroscopy, *Appl. Spectrosc.*, 57, 23-27, 2003.

572 Park, S. S., and Wexler, A. S.: Size-dependent deposition of particles in the human lung at steady-state breathing, *J.*
573 *Aerosol. Sci.*, 39, 266-276, 2008.

574 Pasanen, A. L., Pasanen, P., Jantunen, M. J., and Kalliokoski, P.: Significance of air humidity and air velocity for
575 fungal spore release into the air, *Atmos. Environ.*, 25, 459-462, 1991.

576 Petters, M. D., and Kreidenweis, S. M.: A single parameter representation of hygroscopic growth and cloud
577 condensation nucleus activity, *Atmos. Chem. Phys.*, 7, 1961-1971, 2007.

578 Pope, F. D.: Pollen grains are efficient cloud condensation nuclei, *Environ. Res. Lett.*, 5, 044015, 2010.

579 Posselt, R., and Lohmann, U.: Influence of Giant CCN on warm rain processes in the ECHAM5 GCM, *Atmos.*
580 *Chem. Phys.*, 8, 3769-3788, 2008.

581 Pratt, K. A., DeMott, P. J., French, J. R., Wang, Z., Westphal, D. L., Heymsfield, A. J., Twohy, C. H., Prenni, A. J.,
582 and Prather, K. A.: In situ detection of biological particles in cloud ice-crystals, *Nature Geosci.*, 2, 397-400, 2009.

583 Prenni, A. J., Petters, M. D., Kreidenweis, S. M., Heald, C. L., Martin, S. T., Artaxo, P., Garland, R. M., Wollny, A.
584 G., and Pöschl, U.: Relative roles of biogenic emissions and Saharan dust as ice nuclei in the Amazon basin, *Nat.*
585 *Geosci.*, 2, 401-404, 2009.

586 Prisle, N. L., Lin, J. J., Purdue, S. K., Lin, H., Meredith, J. C., and Nenes, A.: CCN activity of six pollenkits and the
587 influence of their surface activity, *Atmos. Chem. Phys. Discuss.*, 2018, 1-26, 10.5194/acp-2018-394, 2018.

588 Pummer, B. G., Bauer, H., Bernardi, J., Bleicher, S., and Grothe, H.: Suspendable macromolecules are responsible
589 for ice nucleation activity of birch and conifer pollen, *Atmos. Chem. Phys.*, 12, 2541-2550, 2012.

590 Pummer, B. G., Bauer, H., Bernardi, J., Chazallon, B., Facq, S., Lendl, B., Whitmore, K., and Grothe, H.: Chemistry
591 and morphology of dried-up pollen suspension residues, *Journal of Raman Spectroscopy*, 44, 1654-1658, 2013.

592 Reinmuth-Selzle, K., Kampf, C. J., Lucas, K., Lang-Yona, N., Frohlich-Nowoisky, J., Shiraiwa, M., Lakey, P. S. J.,
593 Lai, S. C., Liu, F. B., Kunert, A. T., Ziegler, K., Shen, F. X., Sgarbanti, R., Weber, B., Bellinghausen, I., Saloga, J.,
594 Weller, M. G., Duschl, A., Schuppan, D., and Pöschl, U.: Air Pollution and Climate Change Effects on Allergies in
595 the Anthropocene: Abundance, Interaction, and Modification of Allergens and Adjuvants, *Environ. Sci. Technol.*,
596 51, 4119-4141, 2017.

597 Reponen, T., Willeke, K., Ulevicius, V., Reponen, A., and Grinshpun, S. A.: Effect of relative humidity on the
598 aerodynamic diameter and respiratory deposition of fungal spores, *Atmos. Environ.*, 30, 3967-3974, 1996.

599 Schuttelfield, J., Al-Hosney, H., Zachariah, A., and Grassian, V. H.: Attenuated Total Reflection Fourier Transform
600 Infrared Spectroscopy to Investigate Water Uptake and Phase Transitions in Atmospherically Relevant Particles,
601 *Appl. Spectrosc.*, 61, 283-292, 2007a.

602 Schuttelfield, J. D., Cox, D., and Grassian, V. H.: An investigation of water uptake on clays minerals using ATR-
603 FTIR spectroscopy coupled with quartz crystal microbalance measurements, *J. Geophys. Res.-Atmos.*, 112, D21303,
604 doi: 21310.21029/22007JD008973, 2007b.

605 Shiraiwa, M., Ueda, K., Pozzer, A., Lammel, G., Kampf, C. J., Fushimi, A., Enami, S., Arangio, A. M., Frohlich-
606 Nowoisky, J., Fujitani, Y., Furuyama, A., Lakey, P. S. J., Lelieveld, J., Lucas, K., Morino, Y., Pöschl, U.,

607 Takaharna, S., Takami, A., Tong, H. J., Weber, B., Yoshino, A., and Sato, K.: Aerosol Health Effects from
608 Molecular to Global Scales, *Environ. Sci. Technol.*, 51, 13545-13567, 2017.

609 Skopp, J.: Derivation of the Freundlich Adsorption Isotherm from Kinetics, *J. Chem. Educ.*, 86, 1341, 2009.

610 Sofiev, M., Siljamo, P., Ranta, H., and Rantio-Lehtimäki, A.: Towards numerical forecasting of long-range air
611 transport of birch pollen: theoretical considerations and a feasibility study, *Int. J. Biometeorol.*, 50, 392, 2006.

612 Song, X. W., and Boily, J. F.: Water Vapor Adsorption on Goethite, *Environ. Sci. Technol.*, 47, 7171-7177, 2013.

613 Steiner, A. L., Brooks, S. D., Deng, C. H., Thornton, D. C. O., Pendleton, M. W., and Bryant, V.: Pollen as
614 atmospheric cloud condensation nuclei, *Geophys. Res. Lett.*, 42, 3596-3602, 2015.

615 Stuart, B.: *Infrared Spectroscopy: Fundamentals and Applications*, John Wiley & Sons, Ltd., New York, 2004.

616 Sun, J. M., and Ariya, P. A.: Atmospheric organic and bio-aerosols as cloud condensation nuclei (CCN): A review,
617 *Atmos. Environ.*, 40, 795-820, 2006.

618 Tang, M. J., Cziczo, D. J., and Grassian, V. H.: Interactions of Water with Mineral Dust Aerosol: Water Adsorption,
619 Hygroscopicity, Cloud Condensation and Ice Nucleation, *Chem. Rev.*, 116, 4205–4259, 2016.

620 Tang, M. J., Chen, J., and Wu, Z. J.: Ice nucleating particles in the troposphere: Progresses, challenges and
621 opportunities, *Atmos. Environ.*, 192, 206-208, 2018.

622 Taramarcas, P., Lambelet, C., Clot, B., Keimer, C., and Hauser, C.: Ragweed (*Ambrosia*) progression and its health
623 risks: will Switzerland resist this invasion?, *Swiss Med. Wkly.*, 135, 538-548, 2005.

624 Tong, H. J., Fitzgerald, C., Gallimore, P. J., Kalberer, M., Kuimova, M. K., Seville, P. C., Ward, A. D., and Pope, F.
625 D.: Rapid interrogation of the physical and chemical characteristics of salbutamol sulphate aerosol from a
626 pressurised metered-dose inhaler (pMDI), *Chem. Commun.*, 50, 15499-15502, 2014.

627 Womack, A. M., Bohannan, B. J. M., and Green, J. L.: Biodiversity and biogeography of the atmosphere, *Philos.*
628 *Trans. R. Soc. Lond. Ser. B-Biol. Sci.*, 365, 3645-3653, 2010.

629 Yeh, H. C., Cuddihy, R. G., Phalen, R. F., and Chang, I. Y.: Comparisons of calculated respiratory tract deposition
630 of particles based on the proposed NCRP model and the new ICRP66 model, *Aerosol Sci. Technol.*, 25, 134-140,
631 1996.

632 Yeşilbaş, M., and Boily, J.-F.: Particle Size Controls on Water Adsorption and Condensation Regimes at Mineral
633 Surfaces, *Sci. Rep.*, 6, 32136, doi: 32110.31038/srep32136, 2016.

634 Yin, Y., Levin, Z., Reisin, T. G., and Tzivion, S.: The effects of giant cloud condensation nuclei on the development
635 of precipitation in convective clouds — a numerical study, *Atmos. Res.*, 53, 91-116, 2000.

636